J. Chem. Eng. Data **2007,** *52,* 1209−1212

Thermodynamic Functions of Congruently Melting Compounds Formed in the $CeBr_3$−KBr Binary System

L. Rycerz,[†] E. Ingier-Stocka,[†] M. Berkani,[‡] and M. Gaune-Escard*,[§]

Chemical Metallurgy Group, Faculty of Chemistry, Wroclaw University of Technology, Wybrzeze Wyspianskiego 27, 50-370 Wroclaw, Poland, Laboratoire des Procédés Catalytiques et Thermodynamique des Matériaux, Département de Génie des Procédés, Faculté des Sciences et des Sciences de l'Ingénieur, Université A. Mira de Béjaïa, 06000 Béjaïa, Algérie, and Ecole Polytechnique, Mecanique Energetique, Technopole de Chateau-Gombert, 5 rue Enrico Fermi, 13453 Marseille Cedex 13, France

The heat capacity of the congruently melting compounds K_2CeBr_5 and K_3CeBr_6 was measured by differential scanning calorimetry in the temperature range from 400 K up to 1100 K. A linear heat capacity dependence on temperature was used to fit the experimental data. Through combination of these results with the entropy at 298.15 K, and enthalpies of phase transitions, the thermodynamic functions of K_2CeBr_5 and K_3CeBr_6 were calculated up to $T = 1100$ K.

Introduction

Phase equilibria in lanthanide halide−alkali metal halide systems are generally complex and characterized by the existence of several stoichiometric compounds. The stability of these compounds depends on the nature both of the cations (lanthanide, Ln; alkali, M) and of the halide X.[1−3] Two congruently melting compounds, namely, K_3CeBr_6 and K_2CeBr_5, have been observed in the $CeBr_3$−KBr system.[4]

The present work reports thermodynamic properties (temperatures and enthalpies) of phase transitions as well as the heat capacity ($C^0_{p,\mathrm{m}}$) of these compounds.

Experimental

Chemicals. Cerium(III) bromide was synthesized from cerium(III) carbonate hydrate (Aldrich 99.9 %). $Ce_2(CO_3)_3 \cdot xH_2O$ was dissolved in hot concentrated HBr acid. The solution was evaporated, and $CeBr_3 \cdot xH_2O$ was crystallized. Ammonium bromide was then added, and this wet mixture of hydrated $CeBr_3$ and NH_4Br was first slowly heated to 450 and then to 570 K to remove the water. The resulting mixture was subsequently heated to 650 K for sublimation of NH_4Br. Finally, the salt was melted at 1100 K. Crude $CeBr_3$ was purified by distillation under reduced pressure (~0.1 Pa) in a quartz ampoule at 1150 K. $CeBr_3$ prepared in this way was of a high purity, min 99.9 % (sum of impurities determined by AAS less than 0.1 %). The chemical analysis of cerium was performed by a complexometric titration with standard EDTA. Bromide was determined by an argentometric titration with standard $AgNO_3$ solution. The analytical results are given in Table 1.

Potassium bromide (KBr) was a Merck Suprapur reagent (min 99.9 %). Prior to use, it was progressively heated to fusion under a gaseous HBr atmosphere. HBr in excess was then removed from the melt by argon bubbling.

Table 1. Chemical Analysis of Cerium Bromide

mass %			
Br_{theor}	Br_{exptl}	Ce_{theor}	Ce_{exptl}
63.11	63.09 ± 0.02	36.89	36.91 ± 0.03

The stoichiometric compounds were prepared from $CeBr_3$ and KBr, which were weighed in the molar ratio 3:1 (K_3CeBr_6) or 2:1 (K_2CeBr_5). All the mixtures were prepared in a glovebox filled with purified and water-free argon. Although only a small amount of each sample was used for the differential scanning calorimetry (DSC) experiments (300 to 500 mg), several grams of each compound was synthesized to avoid deviation from stoichiometry. Stoichiometric mixtures of bromides were melted in vacuum-sealed quartz ampoules in an electric furnace. Melts were homogenized by shaking and solidified. These samples were ground in an agate mortar in a glovebox. All chemicals were handled in an argon glovebox with a measured volume fraction of water of about $2 \cdot 10^{-6}$ and continuous gas purification by forced recirculation through external molecular sieves.

Measurements. The temperatures and enthalpies of the phase transitions of K_2CeBr_5 and K_3CeBr_6 compounds were measured with a Setaram DSC 121 differential scanning calorimeter. The apparatus and the measurement procedure have been described in detail previously.[5−6] Samples of 300 to 500 mg were contained in quartz ampoules (about 6 mm diameter, 15 mm length) sealed under a reduced pressure of argon. The sidewalls of the ampoules were grounded to fit the cells snugly into the heat flow detector. Experiments were conducted at heating and cooling rates of 5 $K \cdot min^{-1}$.

Heat capacity was measured with the same Setaram DSC 121 operated in a stepwise mode. This so-called "step method" has already been described.[3,6−9] The heat capacity of the sample was determined over an extended temperature range from two experimental runs in an identical stepwise mode. The first one was registered with two empty cells (containers) of identical mass and the second with one of these cells loaded with the sample. For each heating step, the difference of heat flux between the two series is proportional to the amount of heat (Q_i) necessary to increase the sample temperature by a small

---

* Corresponding author. Tel: +33 491 106882. Fax: +33 491 117439. E-mail: marcelle.gaune-escard@polytech.univ-mrs.fr.
[†] Wroclaw University of Technology.
[‡] Université A. Mira de Béjaïa.
[§] Technopole de Chateau-Gombert.

10.1021/je600517u CCC: $37.00

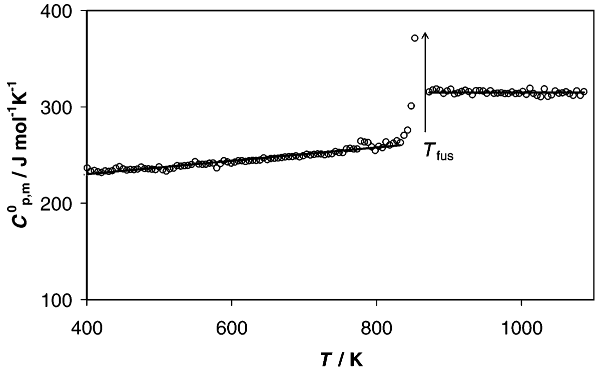

Figure 1. Molar heat capacity $C^0_{p,\mathrm{m}}$ of K_2CeBr_5: ○, mean values from experimental results; solid lines, linear fitting of experimental results.

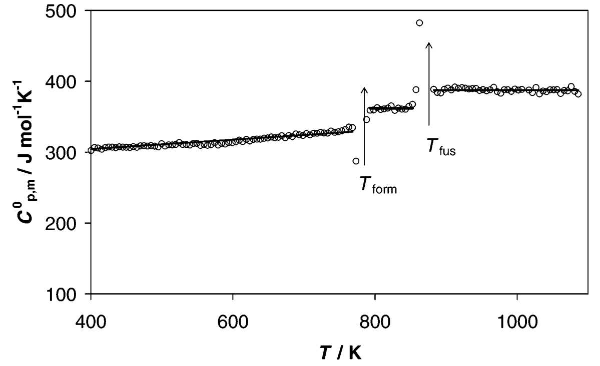

Figure 2. Molar heat capacity $C^0_{p,\mathrm{m}}$ of K_3CeBr_6: ○, mean values from experimental results; solid lines, linear fitting of experimental results.

temperature increment ΔT_i. Therefore, in the absence of any phase transition, the heat capacity of the sample is equal to

$$C_{p,\mathrm{m}} = (Q_i \cdot M_s)/(\Delta T_i \cdot m_s) \tag{1}$$

where m_s is the mass of the sample and M_s is the molar mass of the sample. The same operating conditions (i.e., initial and final temperatures, temperature increment, isothermal delay, and heating rate) were used in the two experimental series. Experimental monitoring, data acquisition, and processing were performed with the Setaram Setsys software.

The DSC 121 apparatus was calibrated by the Joule effect, and some test measurements were performed separately with NIST 720 α-Al_2O_3 Standard Reference material prior to investigation. These tests resulted in $C_{p,\mathrm{m}}$ values consistent with standard data for Al_2O_3 (difference less than 1.5 %), with an exception in the temperature range 300 to 400 K, in which the measured values were significantly larger. The vaporization of the moisture from air condensed on grounded sidewalls of ampoules used in measurements can be given as a tentative explanation of these phenomena. Results of measurements in this temperature range were not taken into account in the polynomial fitting of experimental results.

In the present heat capacity experiments, each 5 K heating step was followed by a 400 s isothermal delay. The heating rate was 1.5 K·min^{-1}. All experiments were performed in the 400 to 1100 K temperature range. The mass difference of the quartz cells in any individual experiment did not exceed 1 mg (cell mass 400 to 500 mg). To establish the repeatability and uncertainty of the results, three different samples of each compound, prepared from different batches, were used in measurements. All these results were used in calculations of coefficients in the equation describing the dependence of heat capacity on temperature as well as the standard deviation on $C^0_{p,\mathrm{m}}$. The maximal deviations of individual series from mean values did not exceed ± 3 % and ± 5 % in the case of K_2CeBr_5 and K_3CeBr_6, respectively.

The linear heat capacity dependence on temperature

$$C^0_{p,\mathrm{m}}/\mathrm{J{\cdot}mol^{-1}{\cdot}K^{-1}} = A + B{\cdot}(T/\mathrm{K}) \tag{2}$$

was fitted to experimental data for both K_2CeBr_5 and K_3CeBr_6. However, because of the strong C_p increase when approaching phase transition or melting, only those data corresponding to a smooth heat capacity dependence on temperature were used.

The $C^0_{p,\mathrm{m}} = f(T)$ equation was then used to calculate enthalpy increments $H^0_\mathrm{m}(T) - H^0_\mathrm{m}(298.15\ \mathrm{K})$ in J·mol^{-1}, entropy $S^0_\mathrm{m}(T)$, and Gibbs energy functions $(G^0_\mathrm{m}(T) - H^0_\mathrm{m}(298.15))/T$ in J·mol^{-1}·K^{-1}, for both the solid and the liquid phase of the compounds under investigation

$$H = H_{298} + \int C_p \mathrm{d}T \tag{3}$$

$$H - H_{298} = AT + 0.5BT^2 + C \tag{4}$$

$$S = S_{298} + \int \frac{C_p}{T} \mathrm{d}T \tag{5}$$

$$S = A \ln T + BT + D \tag{6}$$

$$-(G - H_{298})/T = A \ln T + 0.5BT - CT^{-1} + E \tag{7}$$

The parameters C, D, and E in the above equations were calculated by introduction of T = 298.15 K into eqs 4, 6, and 7. The values of entropy at 298.15 K also necessary in the calculation were obtained by Latimer's method.[10]

Results and Discussion

Enthalpy of Fusion and Heat Capacity of K_2CeBr_5. It was found previously[4] that fusion of K_2CeBr_5 occurs at 874 K with the corresponding enthalpy of 82.4 ± 0.5 kJ·mol^{-1}. Our experimental heat capacity values (mean values from measurements performed on three different samples) of K_2CeBr_5 are plotted against temperature in Figure 1. They were obtained for the first time in this work. The standard deviation of the fitting was 5.24 J·mol^{-1}·K^{-1}. A constant heat capacity value $C^0_{p,\mathrm{m}}$ = 315.01 J·mol^{-1}·K^{-1}, with a standard deviation 3.61 J·mol^{-1}·K^{-1}, was found for liquid K_2CeBr_5.

Thermodynamic Functions of K_2CeBr_5. The thermodynamic functions of K_2CeBr_5 were calculated up to 1100 K using our experimental melting temperature and enthalpy together with the heat capacity data. We determined the $C^0_{p,\mathrm{m}}(K_2CeBr_5, \mathrm{s}, 298.15\ \mathrm{K})$ = 222.66 J·mol^{-1}·K^{-1} by extrapolation of our results to 298.15 K.

The standard entropy $S^0_\mathrm{m}(K_2CeBr_5, \mathrm{s}, 298.15\ \mathrm{K})$ = 378.20 J·K^{-1}·mol^{-1} was obtained by Latimer's method from the empirically found values for the anion and cation contributions.[10]

The $C^0_{p,\mathrm{m}} = f(T)$ equation was then used to calculate enthalpy increments $H^0_\mathrm{m}(T) - H^0_\mathrm{m}(298.15\ \mathrm{K})$ in J·mol^{-1}, entropy $S^0_\mathrm{m}(T)$, and Gibbs energy functions $(G^0_\mathrm{m}(T) - H^0_\mathrm{m}(298.15))/T$ in J·mol^{-1}·K^{-1} for both solid and liquid K_2CeBr_5. The coefficients in corresponding equations and standard errors of their estimation are given in Table 2. The results of these calculations for selected temperatures are presented in Table 3.

Enthalpy of Fusion and Heat Capacity of K_3CeBr_6. K_3CeBr_6 forms at 775 K from KBr and K_2CeBr_5 and melts congruently at 879 K with the related enthalpies 54.5 ± 0.5 and 41.7 ± 0.3 kJ·mol^{-1}, respectively.[4] Our experimental heat capacity data on K_3CeBr_6, obtained for the first time, are plotted against

Table 2. Thermodynamic Functions of K_2CeBr_5 and K_3CeBr_6: Values of *A*, *B*, *C*, *D*, and *E* Parameters in Equations 2, 4, 6, and 7

	temp range	A	$B \cdot 10^3$	$C \cdot 10^{-3}$	D	E
compd	K	$J \cdot mol^{-1} \cdot K^{-1}$	$J \cdot mol^{-1} \cdot K^{-2}$	$J \cdot mol^{-1}$	$J \cdot mol^{-1} \cdot K^{-1}$	$J \cdot mol^{-1} \cdot K^{-1}$
$K_2CeBr_{5(s)}$	298−874	201.51 ± 2.27	70.954 ± 3.561	−62230 ± 831	−791.08 ± 13.99	−989.22 ± 16.25
$K_2CeBr_{5(l)}$	874−1100	315.01 ± 3.61	−	−52930 ± 649	−1403.53 ± 19.96	−1716.32 ± 23.56
$K_3CeBr_{6(s)}$	298−775	272.74 ± 5.20	73.644 ± 8.752	−87860 ± 2330	−1106.62 ± 32.24	−1390.32 ± 38.75
$K_3CeBr_{6(s)}$	775−879	361.90 ± 15.33	−	−58230 ± 4920	−1572.40 ± 92.85	−1916.72 ± 106.09
$K_3CeBr_{6(l)}$	879−1100	387.57 ± 15.05	−	−39090 ± 4680	−1698.97 ± 90.95	−2068.96 ± 103.92

Table 3. Thermodynamic Functions of K_2CeBr_5 at Selected Temperatures (from 298.15 to 1100 K)

T	$C^0_{p,m}(T)$	$S^0_m(T)$	$-(G^0_m(T) - H^0_m(298.15\ K))/T$	$H^0_m(T) - H^0_m(298.15\ K)$
K	$J \cdot mol^{-1} \cdot K^{-1}$	$J \cdot mol^{-1} \cdot K^{-1}$	$J \cdot mol^{-1} \cdot K^{-1}$	$kJ \cdot mol^{-1}$
298.15	222.66	378.20	378.20	0.00
300	222.80	379.58	378.23	0.42
400	229.89	444.64	387.89	23.05
500	236.99	496.70	405.28	46.39
600	244.08	540.54	424.83	70.45
700	251.18	578.70	444.62	95.21
800	258.27	612.70	463.97	120.68
874	263.52	635.78	477.83	139.99
874	315.01	730.06	477.83	222.39
900	315.01	739.29	485.31	230.58
1000	315.01	772.48	512.62	262.08
1100	315.01	802.51	537.83	293.58

Table 4. Thermodynamic Functions of K_3CeBr_6 at Selected Temperatures (from 298.15 to 1100 K)

T	$C^0_{p,m}(T)$	$S^0_m(T)$	$-(G^0_m(T) - H^0_m(298.15\ K))/T$	$H^0_m(T) - H^0_m(298.15\ K)$
K	$J \cdot mol^{-1} \cdot K^{-1}$	$J \cdot mol^{-1} \cdot K^{-1}$	$J \cdot mol^{-1} \cdot K^{-1}$	$kJ \cdot mol^{-1}$
298.15	294.70	469.30	469.30	0.00
300	294.83	471.12	469.24	0.59
400	302.20	556.95	478.17	33.02
500	309.56	625.17	498.78	66.92
600	316.93	682.26	522.91	102.30
700	324.29	731.67	547.71	139.14
775	329.81	764.96	566.09	167.75
775	361.90	835.27	566.09	222.24
800	361.90	846.76	575.23	231.29
879	361.90	880.84	602.77	259.88
879	387.57	928.57	602.77	301.58
900	387.57	937.72	610.89	309.72
1000	387.57	978.56	647.38	348.48
1100	387.57	1015.50	680.76	387.24

temperature in Figure 2. The linear heat capacity dependence on temperature (2) was used to fit the experimental data for solid K_3CeBr_6 in the temperature range 400 to 775 K, with standard deviations 14.12 $J \cdot mol^{-1} \cdot K^{-1}$. In this temperature range, solid K_3CeBr_6 is actually a mixture of solid KBr and K_2CeBr_5 and is denoted "K_3CeBr_6" hereafter. However, because of the strong C_p increase when approaching transitions, only those data corresponding to a smooth heat capacity dependence on temperature were used. Constant heat capacity values, $C^0_{p,m} = 361.90 \pm 15.33\ J \cdot mol^{-1} \cdot K^{-1}$ and $387.57 \pm 15.05\ J \cdot mol^{-1} \cdot K^{-1}$, were found for solid and liquid K_3CeBr_6 in the temperature ranges 775 to 879 K and 879 to 1100 K, respectively.

Thermodynamic Functions of K_3CeBr_6. The thermodynamic functions of K_3CeBr_6 were calculated up to 1100 K using our experimental melting temperature and enthalpy together with the heat capacity data. The value of $C^0_{p,m}(K_3CeBr_6, s, 298.15\ K) = 294.70\ J \cdot mol^{-1} \cdot K^{-1}$, also necessary in these calculations, was obtained by extrapolation of our results to 298.15 K. The standard entropy $S^0_m(K_3CeBr_6, s, 298.15\ K) = 469.30\ J \cdot K^{-1} \cdot mol^{-1}$ was evaluated by Latimer's method.[10]

The parameters in equations for $C^0_{p,m}$ in $J \cdot mol^{-1} \cdot K^{-1}$, $H^0_m(T) - H^0_m(298.15\ K)$ in $J \cdot mol^{-1}$, entropy (S^0_m), and Gibbs energy functions $\{-(G^0_m(T) - H^0_m(298.15))/T\}$ in $J \cdot mol^{-1} \cdot K^{-1}$ dependences on temperature for both solid and liquid K_3CeBr_6 are given in Table 2. The values of thermodynamic functions for selected temperatures are presented in Table 4.

Summary

The heat capacity dependence on temperature was determined for both solid and liquid K_2CeBr_5 and K_3CeBr_6 compounds. These data were used to calculate the whole set of thermodynamic functions up to 1100 K for solid and liquid compounds under investigation.

Literature Cited

(1) Seifert, H. J. Ternary Chlorides of the Trivalent Early Lanthanides. Phase diagrams, Crystal structures and Thermodynamic Properties. *J. Therm. Anal. Calorim.* **2002**, *7*, 789−826.

(2) Rycerz, L. High Temperature Characterization of LnX_3 and LnX_3-AX Solid and Liquid Systems (Ln = Lanthanide, A = Alkali, X = Halide): Thermodynamics and Electrical Conductivity. Ph.D. Thesis, Marseille, 2003.

(3) Rycerz, L. *Thermochemistry of lanthanide halides and compounds formed in lanthanide halide-alkali metal halide systems* (in Polish); Scientific Papers of Institute of Inorganic Chemistry and Metallurgy of Rare Elements, Series Monographs 35; Wroclaw University of Technology: Wroclaw, 2004.

(4) Rycerz, L.; Ingier-Stocka, E.; Gadzuric, S.; Gaune-Escard, M. Phase Diagram and Electrical Conductivity of the $CeBr_3$−KBr Binary System. *Z. Naturforsch.* **2007**, *62a*, 197−204.

(5) Gaune-Escard, M.; Rycerz, L.; Szczepaniak, W.; Bogacz, A. Enthalpies of Phase Transition in the Lanthanide Chlorides $LaCl_3$, $CeCl_3$, $PrCl_3$, $NdCl_3$, $GdCl_3$, $DyCl_3$, $ErCl_3$ and $TmCl_3$. *J. Alloys Compd*. **1994**, *204*, 193−196.
(6) Rycerz, L.; Ingier-Stocka, E.; Cieslak-Golonka, M.; Gaune-Escard, M. Thermal and Conductometric Studies of $NdBr_3$ and $NdBr_3$−LiBr Binary System. *J. Therm. Anal. Calorim.* ***2003***, *72*, 241−251.
(7) Rycerz, L.; Gaune-Escard, M. Heat Capacity of K_3LnCl_6 Compounds with Ln=La, Ce, Pr Nd. *Z. Naturforsch*. **1999**, *54a*, 229−235.
(8) Gaune-Escard, M.; Bogacz, A.; Rycerz, L.; Szczepaniak, W. Heat Capacity of $LaCl_3$, $CeCl_3$, $PrCl_3$, $NdCl_3$, $GdCl_3$, $DyCl_3$. *J. Alloys Compd.* **1996**, *235*, 176−181.
(9) Rycerz, L.; Gaune-Escard, M. Thermodynamics of $SmCl_3$ and $TmCl_3$: Experimental Enthalpy of Fusion and Heat Capacity. Estimation of Thermodynamic Functions up to 1300 K. *Z. Naturforsch*. **2002**, *57a*, 79−84.
(10) Spencer, P. J. Estimation of Thermodynamic Data for Metallurgical Applications. *Therm. Chim. Acta* **1998**, *314*, 1−21.

Received for review November 14, 2006. Accepted April 2, 2007.

JE600517U